

In situ infrared-transmission study of vibrational and electronic properties during the formation of thin-film β -FeSi₂

Cite as: Journal of Applied Physics **91**, 145 (2002); <https://doi.org/10.1063/1.1421041>

Submitted: 09 May 2001 . Accepted: 26 September 2001 . Published Online: 20 December 2001

Gerhard Fahsold, Kilian Singer, and Annemarie Pucci



View Online



Export Citation

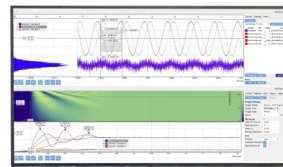
ARTICLES YOU MAY BE INTERESTED IN

[Mechanical properties of layered InSe and GaSe single crystals](#)

Journal of Applied Physics **91**, 140 (2002); <https://doi.org/10.1063/1.1423391>

Challenge us.

What are your needs for periodic signal detection?



Zurich
Instruments

In situ infrared-transmission study of vibrational and electronic properties during the formation of thin-film β -FeSi₂

Gerhard Fahsold,^{a)} Kilian Singer, and Annemarie Pucci

Kirchhoff-Institut für Physik, Ruprecht-Karls-Universität Heidelberg, Albert-Ueberle-Strasse 3-5, D-69120 Heidelberg, Germany

(Received 9 May 2001; accepted for publication 26 September 2001)

Transition metal silicides can be formed by a solid phase reaction of metal films on silicon. During that thermally activated process, the system runs through chemically and crystallographically distinguishable phases with different properties concerning lattice vibrational modes and electronic transport. We demonstrate that *in situ* infrared transmission spectroscopy gives quantitative information on the development of both these properties during formation of the thin-film solid phases. We deposited a 12-nm-thick Fe film on Si(111) and then annealed this system at increasing temperatures. After each step of annealing we measured infrared spectra in normal transmission geometry. The changes in the broadband infrared transmission and the development of vibrational modes allow one to identify the subsequent formation of ϵ -FeSi and polycrystalline β -FeSi₂ and to monitor the interplay of crystalline and electronic structure during formation of these phases. © 2002 American Institute of Physics. [[DOI: 10.1063/1.1421041]

I. INTRODUCTION

The technological interest in thin films with designed electronic properties and thicknesses below a tenth of a micron is continuously increasing. For optoelectronics, photovoltaics, thermoelectrics, and microelectronics, important classes of materials are silicides^{1,2} and oxides.³ Due to the fact that the electronic structure of these materials sensitively depends on stoichiometry and crystalline structure, it may be tuned. Small tetragonal distortions of a cubic lattice, for instance, may lead to a transition from metallic to semiconducting or may alter the type of band gap from direct to indirect. Both effects are substantial for optical applications. The distortions may be spontaneous, i.e., Jahn–Teller-like, may be induced by defects, or may be imposed during a thin-film epitaxial growth process. In any case, when investigating these materials, information on both crystalline and electronic structure is of particular importance. The greatest amount of information can be expected from experiments that deliver this information from the same sample at the same condition (e.g., ambient pressure, temperature, and illumination). Additionally, *in situ* methods allow distortions due to the ambient conditions to be kept at a lower level and offer the possibility of integrating them into a thin-film preparation line. In this article, we propose infrared transmission spectroscopy (IRTS) for this kind of thin film analysis.

In an experiment with solid phase reactions from ultrathin (~ 10 nm) Fe/Si(111) to crystalline silicide films (ϵ -FeSi and β -FeSi₂) we demonstrate the eminent suitability of IRTS as a source of information on thin-film vibrational and electronic properties. We apply IRTS to the sample during successive steps of annealing in ultrahigh vacuum (UHV). This allows monitoring of the development of both crystalline and electronic structure during the phase transitions occurring in

the investigated temperature range. The analysis of the infrared (ir) optical data from the films follows standard procedures,⁴ except for the fact that we also analyze the broadband behavior.⁵ On the experimental side we see an advantage in the normal transmission geometry. Provided that the substrate shows broadband transparency in the investigated ir spectral range, small distortions in the angle of incidence should, compared with reflection geometry, influence the experimental data only weakly.

II. EXPERIMENT

We use a combination of a vacuum Fourier-transform infrared spectrometer (Bruker IFS66v/S) and a UHV chamber (residual pressure $< 2 \times 10^{-10}$ mbar) to perform *in situ* ir spectroscopy on thin-film systems. The setup allows IRTS during preparation of thin films and surfaces under UHV conditions.⁶ Additional surface structure analysis is done by low-energy electron diffraction (LEED).

The Si(111) substrate (Wacker Chemie, $20 \times 20 \times 2$ mm³) is mounted on a molybdenum plate with a central 5-mm aperture for IRTS measurements and with a K-type thermocouple for temperature measurement. For substrate surface preparation this plate is heated to 1100 °C in UHV to desorb the oxide and to form a 7×7 reconstruction. The Fe thin film is prepared with an electron-beam evaporator whose metal-vapor flux hits the substrate surface at an angle of 37.5° with respect to its normal. Substrate temperature is 30 °C. The Fe-film thicknesses are calculated from the deposition rate (0.2 nm/min assuming Fe bulk density), which was calibrated with a quartz microbalance. Silicide formation is enabled by thermal activation during successive annealing periods of 5 min at a temperature T_a . This temperature is raised in steps of $\Delta T_a = 25$ °C to a maximum temperature of 1100 °C. Between these annealing periods,

^{a)}Electronic mail: fahsold@urz.uni-heidelberg.de

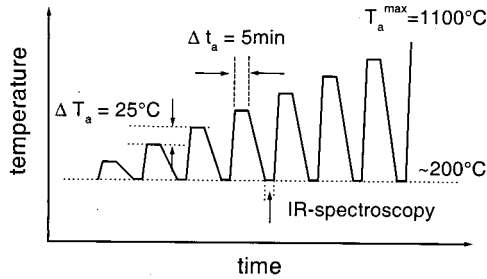


FIG. 1. Subsequent steps of annealing for a duration of 5 min; the annealing temperature T_a is increased in steps of 25 °C to a maximum of 1100 °C. *In situ* ir transmission spectroscopy is done at ~ 200 °C and between the annealing periods.

the sample temperature is lowered to ~ 200 °C to perform IRTS (see Fig. 1).

For this experiment we measured ir transmission from 200 to 2000 cm^{-1} with a resolution of 2 cm^{-1} (all frequencies are given in wave-number units cm^{-1}). An area of ~ 4 mm^2 of the sample surface is illuminated by the ir light at normal incidence. We used a globar ir light source (Bruker), a CsI beam splitter (Bruker), and Si windows (Wacker Chemie) to connect the UHV chamber to the vacuum spectrometer, and a DTGS detector (Bruker) for light detection.

The shown spectra of relative transmission are referenced to the transmission of the bare silicon substrate held at the same temperature as the sample with the thin film under investigation. However, as small differences in these temperatures lead to imperfect compensation and as, in small spectral ranges, the low intensities lead to strong noise in the relative intensities, small sections (700–800 and 1250–1500 cm^{-1}) of the measured spectral range are skipped in the presentation of spectra. For monitoring the spectral changes when annealing the films, typically 100 scans were recorded within ~ 2 min at (200 ± 20) °C to give one spectrum. For a more detailed analysis of the different silicide phases we raised the number of scans to 1000 and measured when the sample had cooled down to (100 ± 5) °C. All measurements were done *in situ* and on the same sample.

III. RESULTS

The result of our ir optical measurement after growth of the Fe thin film is shown in Fig. 2. The spectrum demonstrates that an Fe film of 12.3 nm thickness is still transparent in the mid-ir. This was to be expected from our earlier experiments on silicon and from measurements of Fe thin films on ionic crystal surfaces.^{5,7} The transmission increases with increasing wave number (i.e., positive dispersion) and reaches a value of 20% at 2000 cm^{-1} .

The measured development of ir transmission with increasing annealing temperature T_a is presented in Fig. 3. The spectral range shown gives an overview of both the raising of the broadband baseline and the formation of vibrational structure with increasing T_a . There are two ranges of T_a

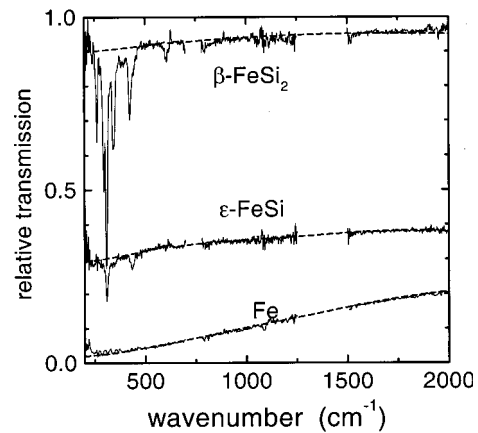


FIG. 2. Relative transmission of as-grown and annealed 12-nm iron on Si(111). The iron film is grown and measured at room temperature. The silicide films are the result of annealing to 675 °C (ϵ -FeSi) and 900 °C (β -FeSi₂); the transmission is measured at 100 °C.

where the optical properties rapidly change: between 475 and 550 °C and between 725 and 800 °C. Remarkably, broadband transmission and vibrational structure seem to develop simultaneously in these ranges. This rough inspection of the series of spectra already allows an identification of three stable phases, which we denote as P0, P1, and P2 for low, intermediate, and high annealing temperature, respectively. It will be revealed in Sec. V that the phases are metal-on-silicon (Fe/Si), monosilicide-on-silicon (ϵ -FeSi/Si), and disilicide-on-silicon (β -FeSi₂/Si), respectively.

The dependence of ir transmission $T(\omega)$ on T_a is given in more detail in Fig. 4. This figure shows the transmission at $\omega = 332$ cm^{-1} and at $\omega = 370$ cm^{-1} , which represent the broadband raise of ir transmission with increasing T_a . The

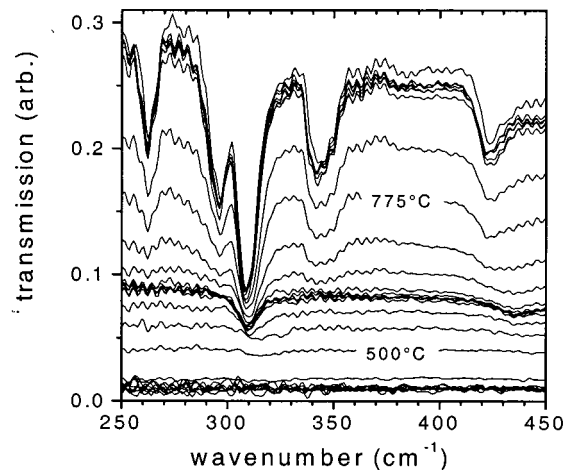


FIG. 3. Development of vibrational structure and broadband transmission after subsequent periods of Fe/Si(111) thin-film annealing. The spectra are measured at ~ 200 °C and the annealing temperature T_a is increased in steps of 25 °C. For two spectra, T_a is indicated (500 and 775 °C). Maximum temperature is 1100 °C. The weak periodic modulation of the spectra is due to interferences from the windows in the optical path.

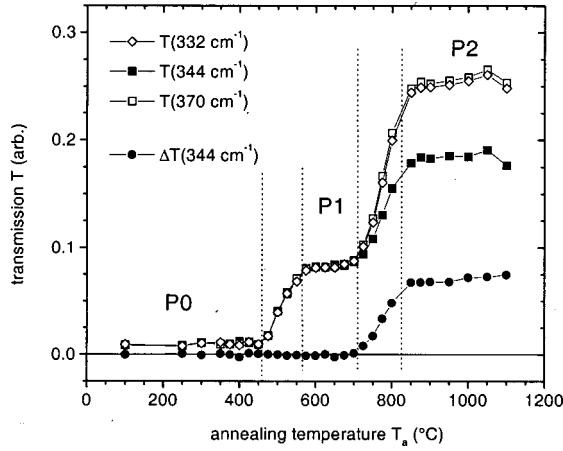


FIG. 4. Development of vibrational structure and broadband transmission with annealing temperature T_a . The transmission $T(\omega)$ is shown for $\omega = 332$ and 370 cm^{-1} to monitor the broadband changes. The development of vibrational structure at $\omega = 344 \text{ cm}^{-1}$ is monitored by the transmission $T(344 \text{ cm}^{-1})$ and by the transmission difference $\Delta T(344 \text{ cm}^{-1}) = T(332 \text{ cm}^{-1}) - T(344 \text{ cm}^{-1})$. P0, P1, and P2 label the existence of stable phases as deduced from the $T(\omega)$ curves.

occurrence of the above-mentioned stable phases P0, P1, and P2 is quite significant. For monitoring the development of vibrational absorption at 344 cm^{-1} , for example, the transmission difference $\Delta T(344 \text{ cm}^{-1}) = T(332 \text{ cm}^{-1}) - T(344 \text{ cm}^{-1})$ is calculated. Clearly, this resonance line appears during only the second transition ($725 \text{ °C} \leq T_a \leq 800 \text{ °C}$), and it remains unchanged (within the errors due to the uncertainty in the sample temperature) up to maximum T_a . The same holds for the strong resonance lines at 263, 297, and 425 cm^{-1} (see Fig. 3).

The spectra for the numerical analysis of the ir optical properties of P1 and P2 are shown in Fig. 2. Together with the spectrum of P0, these spectra show that the phases strongly differ in broadband absorption, i.e., strong metallic absorption in P0, intermediate absorption in P1, and weak absorption in P2. Concurrent with the decrease of broadband absorption a variety of resonance absorption develops, which indicates that delocalized charge carriers are increasingly localized in polarizable chemical bonds. These are preliminary hints of silicide formation.

IV. ANALYSIS OF SPECTRA

For quantitative analysis of our experimental data we perform optical calculations with the commercial software⁸ SCOUT2 which takes account of multiple reflection and coherent superposition of beams in layered structures. We model the complex dielectric functions of the films to describe our ir-optical results. In the following, this is done separately for the broadband transmission and for the vibrational structure. For the film thickness of P1 and P2 we use 23.8 and 38.3 nm which we calculate from the Fe-film thickness (12.3 nm) and the number of Fe atoms per unit volume in bcc-Fe, ϵ -FeSi, and β -FeSi₂, respectively.

A. Broadband transmission

The weak ir optical transmission of the Fe film as grown (phase P0) and the absence of vibrational structure are reminiscent of the strong absorption due to intraband transitions in a metal. Nevertheless, we know that the pure Drude model with the frequency-independent parameters plasma frequency ω_p and relaxation rate $\omega_\tau = 1/\tau$ fails to describe bulk and thin-film optical properties of iron.^{5,7} For example, with $\omega_p = 33\,000 \text{ cm}^{-1}$ and $\omega_\tau = 147 \text{ cm}^{-1}$, as tabulated in standard literature on ir properties of metals,⁹ the transmission is strongly overestimated in the mid-ir. Instead, we use the frequency-dependent parameters $\omega_\tau(\omega)$ and $\omega_p(\omega)$, which we calculate from experimental data on the dielectric function of iron.⁵ In thin films, interfaces and grain boundaries from the growth process are additional sources for electronic relaxation as described by various treatments of the classical size effect.^{5,10} We introduce a thin-film relaxation rate ω_s which we add to the bulk relaxation rate $\omega_\tau(\omega)$. For modeling depolarization effects, which are known for inhomogeneous films,¹¹ for example, we scale the plasma frequency $\omega_p(\omega)$ with a frequency-independent factor⁵ β . Our metal thin-film dielectric function $\epsilon_{bb}(\omega)$ for the broadband properties reads as

$$\epsilon_{bb}(\omega) = \epsilon_\infty - \frac{[\beta \omega_p(\omega)]^2}{\omega^2 + i \omega \cdot [\omega_\tau(\omega) + \omega_s]} \quad (1)$$

We achieved excellent matching of the calculated transmission to the experimental data (see Fig. 2) by setting $\epsilon_\infty = 1$, $\omega_s = 270 \text{ cm}^{-1}$, and $\beta = 1.28$.

For modeling the broadband transmission of the phase P1 we used a dielectric function according to Eq. (1) with $\beta = 1$ and $\omega_s = 0 \text{ cm}^{-1}$. No satisfying accordance could be gained by suppressing a frequency dependence in the Drude parameters. Therefore we introduce a frequency dependence by adding up two Drude-type contributions to the susceptibility. This corresponds to intraband transitions in a two-band model. Due to the lower limit of our spectral range ($\omega > 200 \text{ cm}^{-1}$) and the high temperature (373 K) we cannot exclude a weak binding of charge carriers. Even though high ionic polarizability is known for iron monosilicide at low temperature,¹² we used $\epsilon_\infty = 1$, which seems to be appropriate for this narrow-gap semiconductor at temperature above 300 K.^{12,13} With this model and the parameters for the two Drude susceptibilities given in Table I we get the best spectral agreement with our experimental results (see Fig. 2).

The broadband transmission of P2 is well described with a single Drude-type susceptibility and an ionic polarizability corresponding to ϵ_∞ above unity.^{1,14} The best spectral agreement (see Fig. 2) is found for the values given in Table I. We also tried a two-band model, as used for P1, but no substantial improvement in describing the experimental data could be gained. In particular, the value for ϵ_∞ did not increase significantly.

B. Vibrational structure

The measured ir spectra (see Fig. 5) show the vibrational structure of the phases P1 and P2. For their analysis we assume a dielectric function $\epsilon(\omega)$,

TABLE I. Values of the parameters of the dielectric function: background parameters (ϵ_∞ , ω_p , and ω_τ) and harmonic oscillator parameters (ω_j , S_j , and γ_j). These parameters are used for calculating the ir transmission of the prepared silicide-film phases P1 and P2. All frequencies (ω_j , γ_j , ω_p , and ω_τ) are given in wave-number units (cm^{-1}).

Parameter	Phase P1				Phase P2						
ϵ_∞	1.0				7.4						
ω_p	44 680	6231			3970						
ω_τ	11 720	670			2340						
ω_j	309	342	434		263	297	309	344	388	425	459
S_j	15.9	0.9	3.4		3.6	3.8	10.9	4.0	0.4	1.8	0.1
γ_j	10	15	15		7	7	7	13	21	15	15

$$\epsilon(\omega) = \epsilon_{bb}(\omega) + \sum_j \frac{S_j \cdot \omega_j^2}{\omega_j^2 - \omega^2 - i\omega\gamma_j}, \quad (2)$$

with broadband dielectric properties $\epsilon_{bb}(\omega)$ as described above and with harmonic oscillators with resonance frequency ω_j , oscillator strength S_j , and damping rate γ_j . Our experimental results do not show significant asymmetries in the vibrational absorption lines. Hence we abandon their description by means of Fano-type line shapes.¹² The results from the fit to the experimental data are shown in Table I.

V. DISCUSSION

A. Characterization of thin film phases

1. Phase P0

The used model dielectric function for Fe thin films properly describes the ir optical properties of the iron film as grown. As the electron mean free path in iron varies between 70 and 7 nm in the spectral range under investigation, the weak increase in electronic relaxation in the 12-nm film is consistent with estimations for the classical size effect in a homogeneous film. The found value for the scaling factor β is also observed for homogeneous iron thin films on MgO(001).⁵ This excludes both a strong intermixing of iron at the interface and a strong inhomogeneity due to a pronounced three-dimensional-island growth mode, as known, for instance, from metals on SiO₂-covered silicon.¹⁵

2. Phase P1

The vibrational and electronic data of this phase are consistent with ϵ -FeSi/Si. The harmonic oscillator values for the

vibrational structures agree with the results of Damascelli *et al.*¹² for bulk ϵ -FeSi at room temperature. They found oscillator frequencies of 318, 338, and 445 cm^{-1} with oscillator strengths of 12, 1.5, and 5, respectively. From our broadband analysis we get a real part of the dielectric function which increases from -100 at 100 cm^{-1} to -22 at 2000 cm^{-1} . These values closely match the properties of bulk ϵ -FeSi at 300 K. The same holds for the conductivity. We calculate $3.8 \times 10^{-3} \Omega \text{ cm}$ at 100 cm^{-1} and $8 \times 10^{-3} \Omega \text{ cm}$ at 2000 cm^{-1} , while bulk properties are 3.2×10^{-3} and $2.7 \times 10^{-3} \Omega \text{ cm}$, respectively. The slightly increased conductivity in our experiment should be due to the higher sample temperature (373 K).

We want to comment on the broadband dielectric function of P1, which we identified as ϵ -FeSi. At temperatures below 200 K the conductivity shows distinguishable spectral weight from both intraband transitions and interband transitions across the narrow gap (~ 0.1 eV, i.e., in wave-number units $\sim 1000 \text{ cm}^{-1}$). Above 250 K the spectral separation of these contributions has disappeared, which is connected to the disappearance of the gap around 300 K.¹³ The choice of a two-band charge carrier model with two Drude-type contributions accounts for this situation. Concurrent with the disappearance of the gap the static background polarizability should decrease, i.e., ϵ_∞ should approach a value around unity.

3. Phase P2

The large number of distinct absorption lines points at high crystalline order with a large unit cell. We compared the vibrational structure of P2 with data¹⁶ from the various phases and morphologies of FeSi₂ and found that the best agreement was with polycrystalline^{17,18} β -FeSi₂. For demonstration we calculated a transmission spectrum (see Fig. 5) using the thickness of our films and the vibrational data from 20-nm-thick β -FeSi₂ on Si(111). This film is grown by molecular beam epitaxy (MBE) and is annealed at 660 °C. It is polycrystalline with a preferential orientation perpendicular to the surface.¹⁹ Our films obviously have a slightly stronger polycrystalline character than these MBE films. We deduce this from the $\sim 30\%$ lower strength of the oscillator at 425 cm^{-1} . It is known²⁰ that with increasing polycrystalline character the spectral weight bunches around $\sim 300 \text{ cm}^{-1}$. Concurrently, the density of charge carriers increases.²⁰ From our measured broadband-dielectric properties at 373 K we calculate a density of charge carriers of $1.4 \times 10^{20} \text{ cm}^{-3}$, conductivity of $110 \Omega^{-1} \text{ cm}^{-1}$, and mobility of $5 \text{ cm}^2/\text{V s}$. A

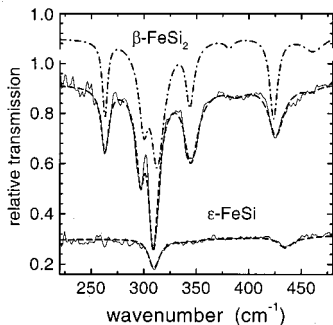


FIG. 5. Relative transmission of silicide thin films: measured at 373 K (solid line), calculated with fitted parameters (dashed line), and calculated with data from MBE films (dash-dotted line).

charge carrier mass of $0.8 m_e$ is assumed for the calculation.²¹ Bearing in mind the temperature of our films, these values are typical¹ for polycrystalline β -FeSi₂. Accordingly, the films of this experiment are still insufficient for most technical applications.

B. Phase transitions

Our *in situ* investigation method allows monitoring of the development of both the free charge carriers and the crystalline structure, which is of high importance in systems of strong electron–phonon coupling and Jahn–Teller-like phase transitions. For the two phase transitions we observe a concurrent change in the broadband absorption and the vibrational absorption structure. Indeed, this is a strong indication for a mutual influence of both the electronic and vibrational properties. We also find that the transitions occur for the complete system and within small temperature ranges. There is no indication for the occurrence of an α -FeSi₂ phase²² or for a gradual change of the Fe–Si stoichiometry which goes from a pure Fe film to a FeSi₂ film over a broad range of temperatures. Such a gradual change could be due to a homogeneous mixture of Fe and Si or to coexistence of two phases. After completion of FeSi₂ formation, we do not observe a further change in β -FeSi₂ properties, in particular in the strength of the oscillator at 425 cm^{-1} . This means that the polycrystalline character is established at 850°C and it remains unchanged up to temperatures above 1100°C . For films of iron on silicon, thinner than 6 nm, and at temperatures above 600°C , the formation of silicide islands is found.²³ The formation of silicide islands is not indicated from our analysis of the broadband behavior.⁵

VI. CONCLUSION AND SUMMARY

With our investigation of the solid phase epitaxy of β -FeSi₂ we demonstrated that infrared transmission spectroscopy (IRTS) is a powerful method for gaining information on the vibrational structure and electronic properties of silicide films with thicknesses far below 100 nm. Within small ranges of annealing temperature the formation of ε -FeSi and polycrystalline β -FeSi₂ could be identified from the measured vibrational absorption lines and the broadband ir transmission. All measurements were done *in situ* and on

the same sample. Hence we propose IRTS for the investigation of further silicide thin film systems.

ACKNOWLEDGMENTS

The authors are indebted to P. Stauss for the samples with MBE-grown β -FeSi₂ thin films, to Wacker Chemie for the silicon substrates, and to S. Ulrich and V. Greim for preparatory work on the Fe/Si system.

- ¹H. Lange, Phys. Status Solidi B **201**, 3 (1997); Thin Solid Films **381**, 171 (2001).
- ²K. P. Homewood, *et al.*, Thin Solid Films **381**, 188 (2000); K. Oyashi, D. Lenson, R. Carius, and S. Mantl, *ibid.* **381**, 194 (2000); H. Katsumata *et al.*, *ibid.* **381**, 244 (2000); Z. Liu, M. Watanabe, and M. Hanabusa, *ibid.* **381**, 262 (2000); A. Heinrich, H. Griessman, G. Behr, K. Ivaneko, J. Schumann, and H. Vinzelberg, *ibid.* **381**, 287 (2000). (2001).
- ³P. A. Cox, *Transition Metal Oxides* (Clarendon, Oxford, 1992).
- ⁴O. Stenzel, *Das Dünnschichtspektrum* (Akademie Verlag, Berlin, 1996).
- ⁵G. Fahsold, A. Bartel, O. Kraut, N. Magg, and A. Pucci, Phys. Rev. B **61**, 14108 (2000).
- ⁶O. Krauth, Ph.D. thesis, Universität Heidelberg, 1999.
- ⁷G. Fahsold, W. Keller, O. Krauth, and A. Lehmann, Surf. Sci. **402–404**, 790 (1998).
- ⁸Software SCOUT2, M. Theiss—Hard- and Software, Aachen, Germany, 2000.
- ⁹M. A. Ordal, R. J. Bell, R. W. Alexander, Jr., L. L. Long, and M. R. Querry, Appl. Opt. **24**, 4493 (1985).
- ¹⁰H. Hoffmann and J. Vancea, Thin Solid Films **85**, 147 (1981).
- ¹¹S. Berthier and K. Driss-Khodja, Opt. Commun. **70**, 29 (1989).
- ¹²A. Damascelli, K. Schulte, D. van der Marel, and A. Menovsky, Phys. Rev. B **55**, R4863 (1997).
- ¹³Z. Schlesinger, Z. Fisk, H. Zhang, M. B. Maple, J. F. DiTusa, and G. Aeppli, Phys. Rev. Lett. **71**, 1748 (1993).
- ¹⁴H. Kakemoto, Y. Makita, Y. Kino, S. Sakuragi, and T. Tsukamoto, Thin Solid Films **381**, 251 (2001).
- ¹⁵H. D. Liu, Y. P. Zhao, G. Ramanath, S. P. Muraka, and G. C. Wang, Thin Solid Films **384**, 151 (2001).
- ¹⁶G. Guizzetti, F. Marabelli, M. Patrini, P. Pellegrino, B. Pivac, L. Miglio, V. Meregalli, H. Lange, W. Henrion, and V. Tomm, Phys. Rev. B **55**, 14290 (1997).
- ¹⁷S. Ulrich, diploma thesis, Universität Heidelberg, 1997.
- ¹⁸A. Borghesi, A. Piaggi, A. Stella, G. Guizzetti, F. Nava, and G. Santoro, in *Proceedings of the 20th ICPS*, edited by E. M. Anastassakis and J. D. Jannopoulos (World Scientific, Singapore, 1991).
- ¹⁹P. Stauss, M. Schmidt, and B. Selle (private communication).
- ²⁰G. Guizzetti, F. Marabelli, M. Patrini, Y. Mo, N. Onda, and H. von Känel, in *Silicides, Germanides, and Their Interfaces* (Materials Research Society, Pittsburgh, 1994).
- ²¹N. E. Christensen, Phys. Rev. B **42**, 7148 (1990).
- ²²A. Toneva, E. Goranova, G. Beshkov, Tsv. Marinova, and A. Kakanakova-Georgieva, Vacuum **58**, 420 (2000).
- ²³J. Chrost, J. J. Hinarejos, P. Segovia, E. G. Michel, and R. Miranda, Surf. Sci. **371**, 297 (1997).